ARTICLE

The presubiculum links incipient amyloid and tau pathology to memory function in older persons

Heidi I.L. Jacobs, PhD, Jean C. Augustinack, PhD, Aaron P. Schultz, PhD, Bernard J. Hanseeuw, MD, PhD, Joseph Locascio, PhD, Rebecca E. Amariglio, PhD, Kathryn V. Papp, PhD, Dorene M. Rentz, PsyD, Reisa A. Sperling, MD, and Keith A. Johnson, MD

Correspondence
Dr. Jacobs
hjacobs@mgh.harvard.edu

Neurology® 2020;94:e1916-e1928. doi:10.1212/WNL.0000000000009362

Abstract

Objective

To identify the hippocampal subregions linking initial amyloid and tau pathology to memory performance in clinically normal older individuals, reflecting preclinical Alzheimer disease (AD).

Methods

A total of 127 individuals from the Harvard Aging Brain Study (mean age 76.22 ± 6.42 years, 68 women [53.5%]) with a Clinical Dementia Rating score of 0, a flortaucipir tau-PET scan, a Pittsburgh compound B amyloid-PET scan, a structural MRI scan, and cognitive testing were included. From these images, we calculated neocortical, hippocampal, and entorhinal amyloid pathology; entorhinal and hippocampal tau pathology; and the volumes of 6 hippocampal subregions and total hippocampal volume. Memory was assessed with the selective reminding test. Mediation and moderation analyses modeled associations between regional markers and memory. Analyses included covariates for age, sex, and education.

Results

Neocortical amyloid, entorhinal tau, and presubiculum volume univariately associated with memory performance. The relationship between neocortical amyloid and memory was mediated by entorhinal tau and presubiculum volume, which was modified by hippocampal amyloid burden. With other biomarkers held constant, presubiculum volume was the only marker predicting memory performance in the total sample and in individuals with elevated hippocampal amyloid burden.

Conclusions

The presubiculum captures unique AD-related biological variation that is not reflected in total hippocampal volume. Presubiculum volume may be a promising marker of imminent memory problems and can contribute to understanding the interaction between incipient AD-related pathologies and memory performance. The modulation by hippocampal amyloid suggests that amyloid is a necessary, but not sufficient, process to drive neurodegeneration in memory-related regions.

From the Department of Radiology (H.I.L.J., A.P.S., K.A.J.), Division of Nuclear Medicine and Molecular Imaging, Department of Radiology (H.I.L.J., J.C.A., A.P.S., B.J.H., R.A.S.), The Athinoula A. Martinos Center for Biomedical Imaging, and Department of Neurology/Biostatistics (J.L., R.A.S., K.A.J.), Massachusetts General Hospital/Harvard Medical School, Boston; Faculty of Health, Medicine and Life Sciences (H.I.L.J.), School for Mental Health and Neuroscience, Alzheimer Centre Limburg, Maastricht University, the Netherlands; Department of Neurology (B.J.H., R.A.E., K.V.P., D.M.R., R.A.S., K.A.J.), Center for Alzheimer Research and Treatment, Brigham and Women's Hospital, Harvard Medical School, Boston, MA; and Department of Neurology (B.J.H.), Cliniques Universitaires Saint-Luc, Institute of Neuroscience, Université Catholique de Louvain, Brussels, Belgium.

Go to Neurology.org/N for full disclosures. Funding information and disclosures deemed relevant by the authors, if any, are provided at the end of the article.

Glossary

AD = Alzheimer disease; **CA** = cornu ammonis; **DVR** = distribution volume ratio; **eTIV** = estimated intracranial volume; **FS** = FreeSurfer; **FTP** = 18F-flortaucipir; **HABS** = Harvard Aging Brain Study; **IQR** = interquartile range; **MTL** = medial temporal lobe; **PiB** = 11C Pittsburgh compound B; **RMSEA** = root mean squared error of approximation; **ROI** = region of interest.

The medial temporal lobe (MTL) is vulnerable to early structural and molecular changes contributing to Alzheimer disease (AD)–related memory deficits. The progression of tau pathology from entorhinal cortices through the distinct hippocampal subregions sequentially[1–3] has been associated with increases in amyloid and tau pathology and the onset of subtle memory deficits in clinically normal individuals.[4] In autopsy studies, a variable combination of tau and amyloid pathology has been reported in individuals who had a Clinical Dementia Rating score of 0 at the time of death. In most of these cases, fibrillar amyloid pathology was absent until Braak III, but when tau tangles reached Braak III (hippocampus) or higher, amyloid pathology was widespread in neocortex and in 55% of these cases also found in the hippocampus.[5,6] These individuals, when clinically normal, represent preclinical AD.[6–8] These autopsy reports mark the hippocampus as a critical nexus of AD pathology. Given these findings and the desire to detect AD as early as possible, we aimed to examine whether pathology in these early affected brain regions can capture relevant cognitive AD-related information. To that end, we associated patterns of initial deposition of amyloid (neocortex, hippocampus, and entorhinal) and tau (entorhinal cortex and hippocampus) with memory performance in 127 clinically normal older individuals. Hippocampal tau measurements are confounded by off-target binding from the choroid plexus.[9] Therefore, we focused on hippocampal subfield volumes, which have differential vulnerabilities to aging and AD, consistent with progression of amyloid and tau along the subfields during disease progression.[10]

Methods

Participants

Clinically normal older individuals from the Harvard Aging Brain Study (HABS) who underwent 3T MRI, ^{18}F-flortaucipir (FTP), and ^{11}C Pittsburgh compound B (PiB)-PET were included (n = 127, mean age 76.22 [SD 6.42] years). Participants were included if they had a Clinical Dementia Rating score of 0 and a Mini-Mental State Examination score ≥25. Because this study focused on cross-sectional associations, the time between the FTP-PET visit, PiB-PET visit, MRI, or cognitive assessment was maximally 1 year. All participants underwent at least 1 comprehensive medical and neurologic evaluation and had no medical or neurologic disorders that could contribute to their cognitive abilities. Presence of clinical depression (as measured by the Geriatric Depression Scale) or other psychiatric illnesses, history of alcoholism, drug abuse, or head trauma was an exclusion criterion. A blood sample was obtained to assess *APOE* genotype. Analyses for this study were done between January 2016 and January 2017.

Standard protocol approvals, registrations, and patient consents

Study protocols were approved by the Partners Human Research Committee of Massachusetts General Hospital, and all participants provided written informed consent.

Structural MRI

MRI was performed at the Athinoula A. Martinos Center for Biomedical Imaging on a 3T Trim Trio system (Siemens, Malvern, PA). Structural T1-weighted magnetization-prepared rapid-acquisition gradient-echo images were collected (repetition time 2,300 milliseconds, echo time 2.95 milliseconds, inversion time 900 milliseconds, flip angle 9°, 1.05 and 1.05 × 1.05 × 1.20–mm resolution).

T1-weighted images were processed with FreeSurfer (FS) version 6.0 using the default, automated reconstruction protocol of the software package as described previously.[11] The hippocampal segmentation algorithm in FS 6.0 predicts the location of hippocampal subregions by using a probabilistic atlas built from a combination of manual delineations of the hippocampal formation from 15 ultra-high-resolution (120 μm^3), ex vivo MRI scans showing definitive borders and manual annotations of surrounding subcortical structures (e.g., amygdala, cortex) from an independent dataset of 39 in vivo 1-mm T1 MRI scans.[12] We visually inspected and, if necessary, edited for overestimation or underestimation of gray/white matter boundaries and to identify brain areas erroneously excluded during skull stripping. In addition, we checked that the hippocampal subregion mask was well positioned. Finally, we checked the ranking of the subregion volumes. For the subregions of interests, cornu ammonis (CA) 1 volume was expected to be largest and CA3 the smallest. In 12 participants, the presubiculum was the smallest, and on further inspection, we did not notice any issues in these segmentations.

For the current study, we focused on the subiculum, presubiculum, CA1, CA2/3, CA4, and dentate gyrus (figure 1). Volumes for left and right hippocampal subregions were added. Total hippocampal volume consisted of the sum of all subregions and the tail of the hippocampus.

Every volume was adjusted for the estimated intracranial volume (eTIV) with the following equation:

Figure 1 Depiction of the hippocampal subregions as segmented by FreeSurfer

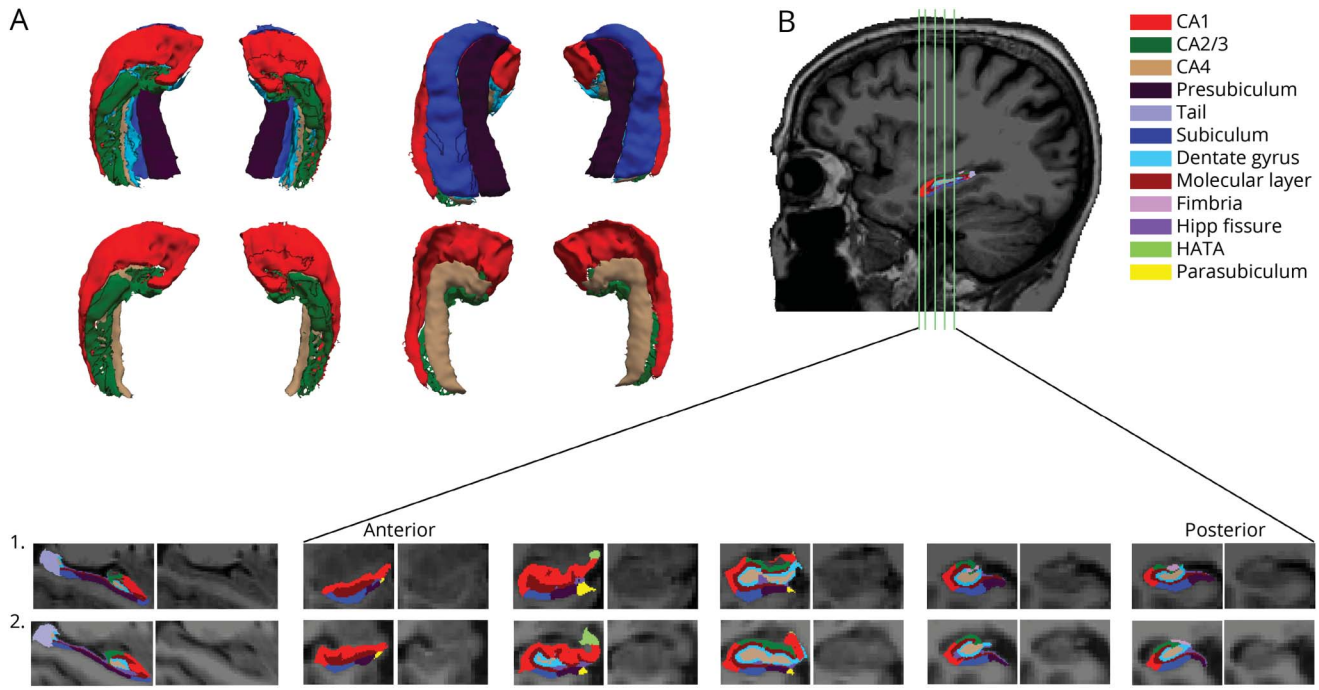

Because the cornu ammonis (CA) 4 is not very visible in the top of row (A) (hidden under subiculum and presubiculum), we also created surfaces of only the CA regions. (B) Overall sagittal and coronal views of the subregions from anterior to posterior (locations are indicated with green vertical lines on the sagittal view). The first participant is a patient with lower levels of amyloid deposition (frontal, lateral temporal, and retrosplenial cortices [FLR] = 1.152 distribution volume ratio [DVR]). The second participant represents an individual with elevated amyloid deposition (FLR = 2.762 DVR). HATA = hippocampal amygdala transition area.

$$\begin{aligned}&\text{Adjusted hippocampal (subfield) volume}\\&= \text{raw hippocampal(subfield)volume}\\&- b(\text{eTIV} - \text{Mean eTIV}),\end{aligned}$$

where b indicates the unstandardized regression coefficient when hippocampal volume is regressed against eTIV. Results reported remain similar when raw volumes are used and intracranial volume is added as a covariate to the model.

Because combining T1 with high-resolution T2 images results in a more accurate segmentation of hippocampal subregions, we evaluated a T1-based vs a T1- and T2-weighted pipeline on an independent dataset of older individuals (n = 130). Volumes of both pipelines correlated highly (r = 0.87–0.97), with the combined pipeline generating consistently greater volumes for all subregions (figure e-1, doi.org/10.5061/dryad.f33n0s8).

Positron emission tomography

The PiB-PET and FTP-PET data were acquired at Massachusetts General Hospital as previously reported[13]: PiB-PET was acquired with a 8.5- to 15-mCi bolus injection followed immediately by a 60-minute dynamic acquisition in 69 frames (12 × 15 seconds, 57 × 60 seconds, 2.6 × 2.6 × 2.4–mm resolution), and FTP was acquired from 80 to 100 minutes after a 9.0- to 11.0-mCi bolus injection in four 5-minute frames on a Siemens/CTI ECAT HR1 scanner. PET data were reconstructed and attenuation corrected, and each frame was evaluated to verify adequate count statistics and absence of head motion.

To evaluate the anatomy of cortical FTP binding, each individual PET dataset was rigidly coregistered to the participant's magnetization-prepared rapid-acquisition gradient-echo imaging data. The FS regions of interest (ROIs) were transformed into PET native space. PiB-PET data were expressed as the distribution volume ratio (DVR) with cerebellar gray as reference tissue using the Logan graphic method applied to data from 40 to 60 minutes after injection.[14] PET data were partial volume corrected with the Geometrical Transfer Matrix method as implemented in FS[15] and with a combination of aseg and aparc parcellations. Neocortical PiB retention was assessed by use of a large cortical ROI aggregate that included frontal, lateral temporal, and retrosplenial cortices. We also assessed hippocampal and entorhinal amyloid deposition (figure e-2, doi.org/10.5061/dryad.f33n0s8, provides an evaluation of the signal-to-noise ratio of these regions). Hippocampal amyloid and entorhinal amyloid were included because seminal neuropathologic staging models of amyloid[16,17] and the National Institute on Aging–Alzheimer's Association guidelines for autopsy studies[6] all agree that MTL regions (hippocampus, entorhinal; phase 2) are affected after the neocortex (phase 1) and before the striatum (phase 3). Autopsy work zooming in on the MTL reported diffuse plaques in the molecular layer of the entorhinal cortex, fleecy amyloid in the CA1, and diffuse plaques in the parvopyramidal layer of the presubiculum during phase 2, indicating that these regions follow neocortical involvement.[18]

While PiB binding to diffuse plaques is weaker,[19,20] it is important to acknowledge that diffuse plaques often contain amyloid fibrils,[21] and even a weak PET signal may reflect substantial underlying amyloid pathology.

Amyloid status was ascertained by a previously determined cutoff based on gaussian mixture modeling approach cutoff value of 1.324. On the basis of this cutoff, 38 individuals (30.89%) were classified with elevated amyloid and 85 (69.11%) with low amyloid. FTP binding was expressed in FS-defined entorhinal cortices, hippocampi, and choroid plexus (left and right were combined into 1 ROI) as the standardized uptake value ratio with cerebellar gray used as reference. To correct hippocampal FTP binding for spill-in signal from the choroid plexus, we created a partial residual adjusting hippocampus signal for choroid plexus signal.[9]

Memory scores

A memory compound score was created by calculating the mean of the *z*-transformed scores of the total recall and delayed recall scores of the Buschke 6-trial Selective Reminding Test. Because FTP-PET was introduced in year 4 for most participants, we created a partial residual adjusted for number of times an individual had taken the test before the date of the memory scores used here. The Selective Reminding Test provides a sensitive indirect measure of hippocampal health in older individuals.[22]

Experimental design and statistical analyses

Statistical analyses were performed with R version 3.3.0 (R Institute for Statistical Computing, Vienna, Austria). Group characteristics are presented as median and interquartile range (IQR). The threshold for statistical significance was set at $p < 0.05$. Missing data were list-wise deleted for the relevant analyses.

Correlations were examined between regional amyloid, tau, hippocampal subfield volume, demographics, and memory. Pearson product-moment correlations were used for continuous variables, and point-biserial correlations were used for dichotomous variables. Then we performed partial correlations (partialling out age, sex, and education) between memory, hippocampal subregion volumes (compared with Fisher *r*-to-*z* transformation), entorhinal tau, hippocampal tau, and hippocampal and neocortical amyloid pathology. Because off-target binding from choroid plexus confounds hippocampal tau measures and may dilute associations with memory,[9] we provided only summary statistics for this measure; we did not include it in our statistical models.

From these correlations, we selected the hippocampal subregions for the following mediation/moderation analyses. Guided by histopathologic studies, we set out stepwise mediation-moderation models to investigate associations between entorhinal tau, amyloid, hippocampal subregion volume, and memory.[23] In a first step, we investigated whether entorhinal tau mediates the association between neocortical amyloid pathology and memory. We compared this to an alternative model in which neocortical amyloid pathology mediates the relationship between entorhinal tau and memory. Sensitivity analyses were done with the E-values approach.[8]

We then investigated whether the selected hippocampal subregion volume mediates the relationship between neocortical amyloid and memory via entorhinal tau (or the alternative model). Finally, we investigated whether hippocampal or entorhinal amyloid influences the relationship between entorhinal tau and hippocampal subregion volume (mediation vs moderation). The Johnson-Neyman technique was used to determine the region of significance of moderation effects by calculating the value at which the moderator produces the α value of 0.05. All models were corrected for age, education, and sex. The model fit of the final model (pruned for covariates when $p > 0.20$) was assessed with the root mean squared error of approximation (RMSEA; <0.05 with a nonsignificant p value of the close fit test) and the Tucker-Lewis Index (>0.95). No adjustment for multiple comparisons was performed.

Data availability

Baseline data from HABS are publicly available online (nmr.mgh.harvard.edu/lab/harvardagingbrain/data). Follow-up data are expected be released.

Results

Sample characteristics

The median age of the participants (n = 127; n = 124 for amyloid measures) was 74.75 years (IQR 70.75–81.25 years), and median education was 16 years (IQR 12.5–18 years). Sixty-eight participants (53.54%) were female, and 37 (30.58%) carried the *APOE* ε4 allele (missing data n = 6). The median neocortical PiB-DVR was 1.215 (IQR 1.151–1.505); in the hippocampus, 1.170 (IQR 1.119–1.233); and in the entorhinal cortex, 1.123 (IQR 1.008–1.235). For the PiB measurements, data for 4 people were not available (n = 123). Thirty-eight individuals (30.89%) had elevated neocortical amyloid (>1.324 DVR). The median FTP standardized uptake value ratio for the entorhinal cortex was 1.288 (IQR 1.141–1.496) and for the hippocampus (adjusted) was 1.078 (IQR 0.957–1.164).

The median score on the adjusted memory composite was 0.114 (IQR −0.873 to 0.849). The median time between MRI and FTP-PET measurements was 118 days (IQR 52.0–149 days). The median time between the memory test and MRI was 39 days (IQR 14.0–181.0 days) and between the memory test and FTP-PET measurements was 81 days (IQR 59.50–121.50 days).

Regional tau and amyloid associations with hippocampal subregion volumes and memory

Unadjusted correlations among hippocampal subregion volumes, age, memory, tau, and amyloid measures are provided in

table 1. When adjusting for age, education, and sex, we observed moderate correlations between presubiculum volume and memory performance ($r = 0.29$, $p = 0.001$) and not with subiculum ($r = 0.14$, $p = 0.133$), CA1 ($r = 0.01$, $p = 0.91$), CA3 ($r = -0.02$, $p = 0.86$), CA4 ($r = 0.05$, $p = 0.55$), dentate gyrus volume ($r = 0.03$, $p = 0.75$), or total hippocampal volume ($r = 0.09$, $p = 0.31$). Presubiculum-memory correlations differed from CA1-, CA3-, CA4-, and dentate gyrus–memory correlations (Fisher $z = 2.27$, $p = 0.023$; $z = 2.19$, $p = 0.028$; $z = 1.96$, $p = 0.05$; $z = 2.11$, $p = 0.035$, respectively) but not from the subiculum-memory correlations (Fisher $z = 1.24$, $p = 0.21$).

Entorhinal tau, adjusted hippocampal tau, and neocortical amyloid deposition correlated moderately with memory (partial $r = -0.25$, $p = 0.006$; $r = -0.18$, $p = 0.044$; $r = -0.24$, $p = 0.01$, respectively, figure 2 and figure e-3, doi.org/10.5061/dryad.f33n0s8). Hippocampal and entorhinal amyloid deposition correlated nonsignificantly with memory performance (hippocampus partial $r = -0.12$, $p = 0.19$; entorhinal partial $r = -0.11$, $p = 0.24$). Partial correlations showed that presubiculum ($r = -0.30$, $p = 0.0007$), subiculum ($r = -0.34$, $p = 0.0001$), CA1 ($r = -0.19$, $p = 0.035$), and total hippocampal volumes ($r = 0.26$, $p = 0.003$) were negatively correlated with entorhinal tau. None of the hippocampal subregion or total hippocampal volumes correlated significantly with neocortical, entorhinal, or hippocampal amyloid deposition before or after correction for age, education, and sex.

Associations between amyloid, tau, hippocampal subregion volume, and memory

Because the presubiculum was the only subregion correlating with memory performance after correction for age, the following hierarchical analyses were performed only for the presubiculum. First, on the basis of histopathologic data, we investigated whether entorhinal tau mediates the relationship between neocortical amyloid deposition and memory. In the alternative model, we tested whether neocortical amyloid deposition mediated the relationship between entorhinal tau and memory. These analyses were performed in 123 individuals (excluding 4 with missing PiB data).

Neocortical amyloid was negatively associated with memory (total effect: $\beta = -0.21$, $z = -2.28$, $p = 0.023$). The indirect effect on the first mediation model was not significant ($p = 0.056$). However, because the standardized estimate between neocortical amyloid and entorhinal tau ($\beta = 0.464$) has a larger effect (>2.5 times) than the entorhinal tau–memory association ($\beta = -0.181$), mediation by entorhinal tau is likely more proximal to neocortical amyloid than to memory performance. Proximal mediation is usually associated with less power for detecting mediation effects, but we observed a significant proportion mediated ($\beta = 0.404$ [0.032–1.45], $p = 0.040$). This was also reflected in the Aroian Sobel test (-1.967, $p = 0.049$, figure 3B and table 2). Sensitivity analyses showed a moderately strong E value of 3.23, indicating that an unmeasured confounder associated at 3.23-fold with each memory and neocortical amyloid could explain away the mediation of $\beta = -0.181$, but a weaker confounder cannot.

We then assessed the alternative model (figure 4). Entorhinal tau was negatively associated with memory (total effect: $\beta = -0.23$, $z = -3.07$, $p = 0.002$), but the indirect effect was not significant (indirect effect $p = 0.20$). These models indicate that greater entorhinal tau explains the association between greater amyloid deposition and lower memory performance, although the mediation effect is weak.

We then introduced presubiculum volume into the model (figure 3C) and found that the total indirect effect for the mediation by presubiculum volume via entorhinal tau is significant ($p = 0.040$). In addition, presubiculum mediated the relationship between entorhinal tau and memory partially (indirect effect: $\beta = -0.08$, $z = -2.36$, $p = 0.018$). This indicates that greater entorhinal tau and lower presubiculum volume mediate the negative association between neocortical amyloid and memory. This also implies that presubiculum volume partially mediates the relationship between entorhinal tau and memory performance.

In the third step, we examined whether hippocampal or entorhinal amyloid mediated or moderated the relationship between entorhinal tau and presubiculum volume. Hippocampal and entorhinal amyloid deposition cannot be mediators because they were not significantly correlated with presubiculum volume (hippocampus partial $r = -0.03$, $p = 0.76$, entorhinal partial $r = -0.09$, $p = 0.28$). Hippocampal amyloid moderated the relationship between entorhinal tau and presubiculum volume such that higher levels of entorhinal tau are associated with lower presubiculum volumes in participants with higher levels of hippocampal amyloid (figure 3D). Applying the Johnson-Neyman technique showed that this occurs at values of 1.1272 hippocampal amyloid DVR and higher ($t[115] = -1.981$, $p = 0.05$, 95% confidence interval −0.929 to 0.000; covariates: neocortical amyloid, age, sex, education, figure 3E). This region of significance was calculated from the interaction and is not comparable to the neocortical amyloid cutoff. In our study, 87 participants (68.5%) have hippocampal amyloid deposition values above this DVR. This includes 32 individuals with elevated neocortical amyloid (or 84.2% of the individuals with elevated levels in the total sample) and 55 individuals with lower neocortical amyloid (or 65% of the individuals with lower levels in the total sample). We also assessed whether hippocampal amyloid affects the strength of the double mediation in step 2. The overall conditional indirect effect estimates (table 2) show that greater entorhinal tau and lower presubiculum volumes explain the relationship between neocortical amyloid deposition and memory performance when hippocampal amyloid levels are elevated (above ≈1.223 DVR). The final model (figure 3D) showed an RMSEA < 0.01 with $p_{close} = 0.96$ and Tucker-Lewis Index of 1.080, an indication that the model described the data well (figure e-4, doi.org/10.5061/dryad.f33n0s8: 10,000 random resamples provided good model fit for 97.4% of the samples). Entering entorhinal amyloid as

Table 1 Correlation matrix of all variables

	1	2	3	4	5	6	7	8	9	10	11	12	13	14	15	16
1. Age	1															
2. Sex	−0.05	1														
3. Educ	−0.07	−0.04	1													
4. Presub	−0.49[c]	0.03	−0.02	1												
5. Sub	−0.50[c]	0.02	−0.05	0.78[c]	1											
6. CA1	−0.43[c]	−0.02	0.03	0.54[c]	0.83[c]	1										
7. CA2/3	−0.38[c]	0.003	−0.09	0.26[b]	0.55[c]	0.8[c]	1									
8. CA4	−0.44[c]	0.03	−0.05	0.46[c]	0.75[c]	0.89[c]	0.92[c]	1								
9. DG	−0.50[c]	0.04	−0.04	0.52[c]	0.79[c]	0.90[c]	0.89[c]	0.98[c]	1[c]							
10. Total HC	−0.54[c]	−0.03	−0.01	0.69[c]	0.91[c]	0.94[c]	0.79[c]	0.92[c]	0.93[c]	1						
11. EC tau	0.26	0.07	0.10	−0.38[c]	−0.42[c]	−0.28[b]	−0.15	−0.22[a]	−0.26[b]	−0.35[c]	1					
12. Res Hipp tau	0.38[c]	−0.01	−0.06	−0.47[c]	−0.47[c]	−0.37[c]	−0.27[b]	−0.37[c]	−0.40[c]	−0.46[c]	0.61[c]	1				
13. Cort amyloid	0.15	0.09	0.03	−0.17	−0.16	−0.15	−0.11	−0.12	−0.14	−0.17	0.50[c]	0.20[a]	1			
14. Hipp amyloid	0.34[c]	−0.008	−0.07	−0.19[a]	−0.18[a]	−0.18[a]	−0.11	−0.13	−0.15	−0.21[a]	0.27[b]	0.24[b]	0.44[c]	1		
15. EC amyloid	0.06	0.15	−0.10	−0.11	−0.12	−0.13	−0.09	−0.11	−0.14	−0.14	0.32[c]	0.13	0.31[c]	0.41[c]	1	
16. Memory	−0.25[b]	0.36[c]	0.17	0.34[c]	0.21[a]	0.10	0.06	0.14	0.14	0.20[a]	−0.22[a]	−0.24[b]	−0.20[a]	−0.19[a]	−0.08	1

Abbreviations: CA = Cornu Ammonis; cort amyloid = neocortical amyloid burden; DG = dentate gyrus; EC = entorhinal cortex; Educ = education; HC = hippocampus; Presub = presubiculum; Res Hipp = partial residual of hippocampal signal; Sub = subiculum.
Values represent Pearson product-moment correlation coefficients between all continuous variables and point-biserial correlations with dichotomous variables (sex).
[a] $p < 0.05$.
[b] $p < 0.01$.
[c] $p < 0.001$.

Figure 2 Relationships between early biomarkers and memory performance

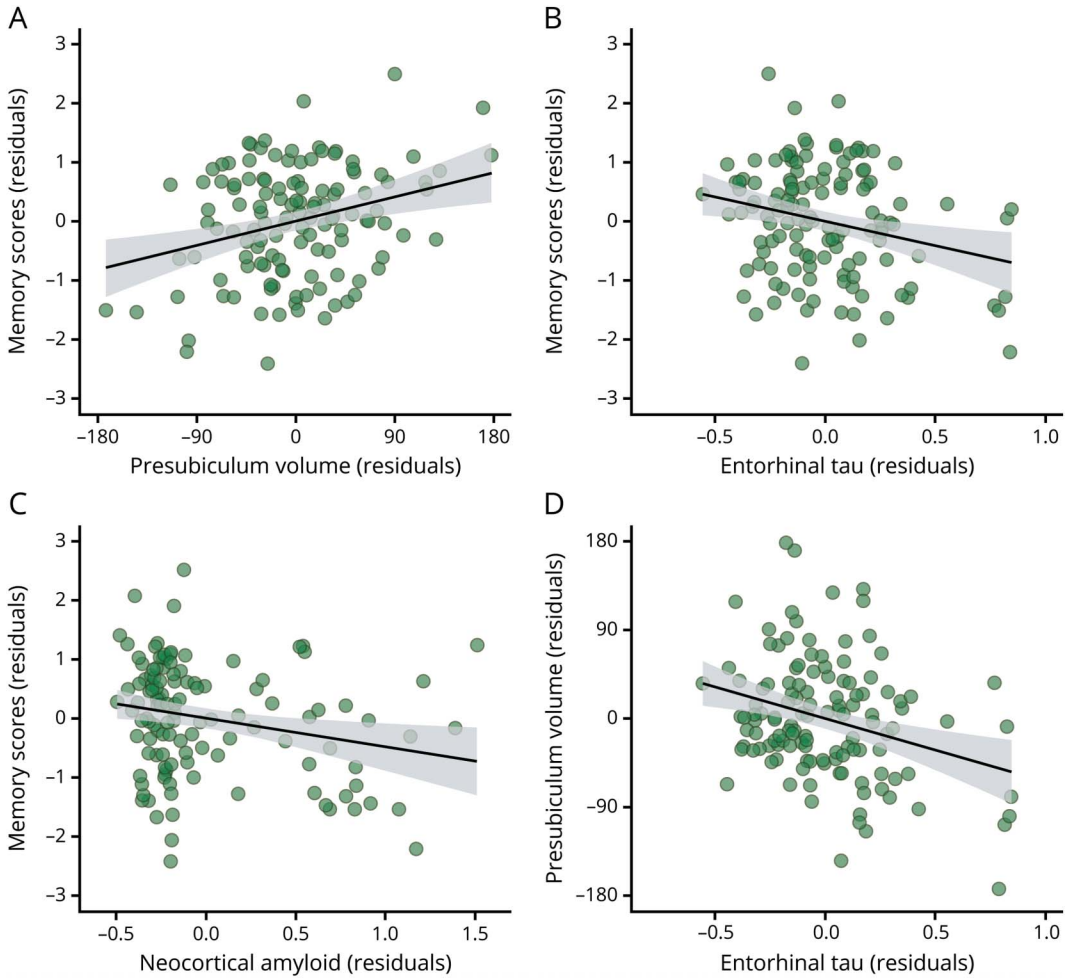

Residualized regressions between (A) presubiculum volume, (B) entorhinal tau, and (C) neocortical amyloid and memory performance, as well as between (D) entorhinal tau and presubiculum volume.

a moderator between entorhinal tau and presubiculum volume resulted in a poor model (RMSEA = 0.61, $p_{close} < 0.01$, table 2). The indirect effect was not contingent on entorhinal amyloid.

To visualize the contributions of the 3 markers (presubiculum volume, neocortical amyloid, and entorhinal tau) to predict memory, we plotted their effect sizes (standardized β coefficients, figure 5). When all markers are in the model (corrected for age, education, and sex), presubiculum volume has the strongest effect size and explains unique variance in memory performance that is not shared with the other markers. These effect sizes were observed for the total sample and were consistent with the path analyses in individuals with elevated hippocampal amyloid. Similar effect sizes were plotted for total hippocampal volume for comparison. Hippocampal volume estimates were not significant in any of the examined groups, indicating that hippocampal volume does not explain any additional variance in memory performance above that of the other biomarkers (note that the negative estimate and larger confidence interval in the low hippocampal amyloid group reflect the small effect and sample size).

Discussion

In the current study, we tested a comprehensive biomarker model that captures the initial pathophysiologic features of preclinical AD and showed that the presubiculum is a critical region, carrying unique information, for understanding the interaction between initial AD-related pathologies and memory performance. More specifically, we showed that in individuals with higher levels of hippocampal amyloid deposition, a combination of higher levels of entorhinal tau and lower presubiculum volume provides the optimal model relating neocortical amyloid deposition to lower memory performance in clinically normal older individuals. Processes underlying tissue loss in the presubiculum may include perforant pathway degeneration caused by higher levels of entorhinal tau or a reduced ability of neurons to integrate and propagate information

Figure 3 Mediation of neocortical amyloid and memory by EC tau and presubiculum volume is contingent on hippocampal amyloid

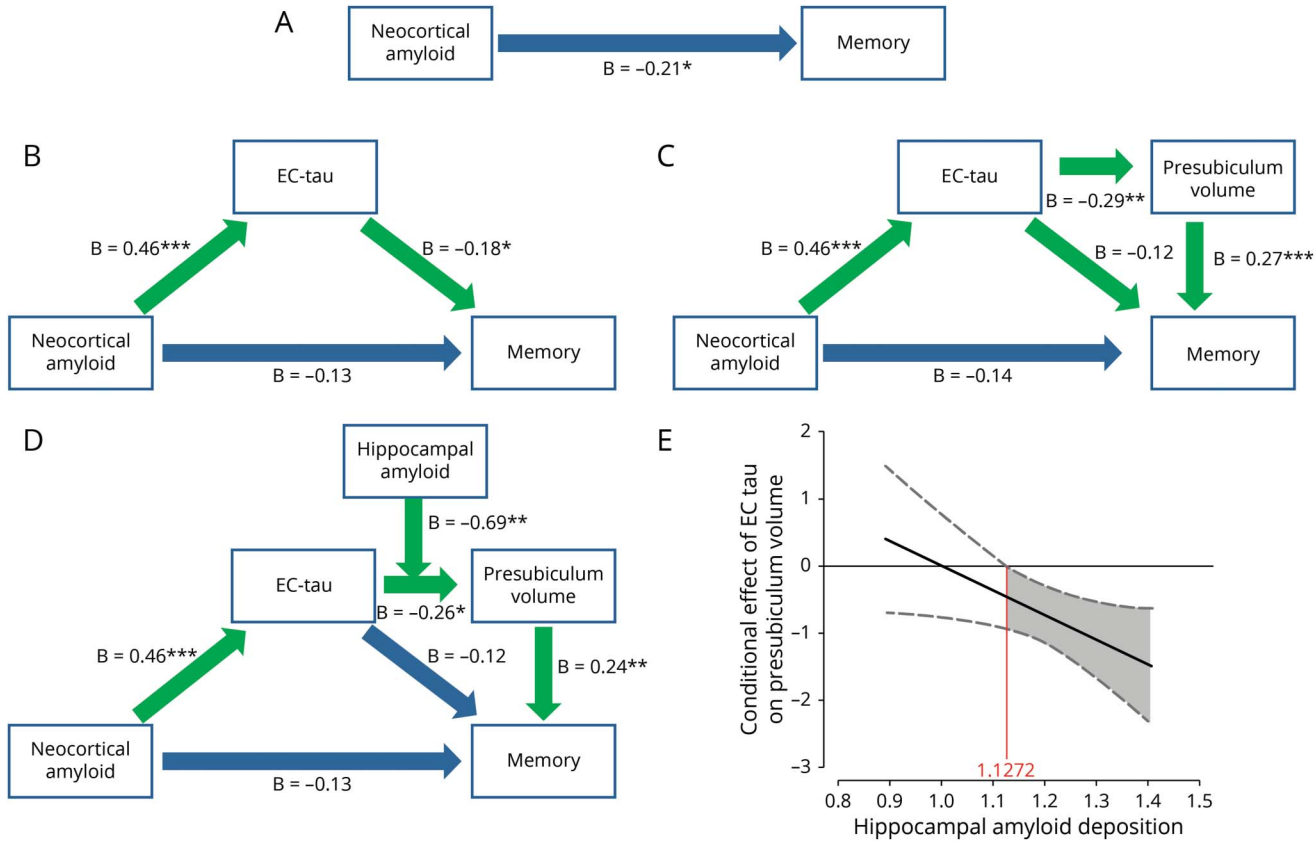

(A) Total effect of neocortical amyloid predicting memory. (B) Mediation by entorhinal cortex (EC) tau and (C) secondary mediation by presubiculum volume. (D) Moderated mediation model. All β values are standardized estimates. (E) Conditional effect by which hippocampal amyloid moderates the mediation of EC tau binding on presubiculum volume. The plot shows that, at higher levels of hippocampal amyloid, the relationship between EC tau and presubiculum volume is more negative compared to lower levels of hippocampal amyloid deposition. Green arrows indicate the significant paths resulting in mediation/moderation. *$p < 0.05$; **$p < 0.01$; ***$p < 0.001$.

under the influence of elevated hippocampal amyloid pathology. These observations are consistent with a pathophysiology of AD in which amyloid pathology is closely related to both tau deposition and presubiculum atrophy as memory loss occurs; however, serial observations will be required to verify the biomarker sequence.

The presubiculum was the only hippocampal subregion associated with memory performance, even surpassing contributions of entorhinal tau or neocortical amyloid pathology. The fact that total hippocampal volume did not predict memory performance, when age or other biomarkers were taken into account, may indicate that presubiculum volume may be an earlier marker of AD pathology, maybe even before changes in total hippocampal volume. Recent animal work indicated that recall of scenes was associated with specifically presubiculum activity.[24] The specificity of our memory findings is consistent with the idea that presubiculum/subiculum subregions are thought to be involved in retrieval processes. Recent work also showed that the presubiculum and subiculum volumes outperformed total hippocampal volume in terms of its diagnostic sensitivity and specificity to differentiate patients with mild cognitive impairment, for whom declarative memory tests were part of the diagnostic workup, from patients with AD.[25] The presubiculum is anatomically an important region; it lies between the entorhinal cortex and CA1, the input and output regions of the hippocampal circuit.[26] This is also consistent with our findings that the presubiculum and CA1 volume correlated with entorhinal tau.

Thus, presubiculum volume links entorhinal tau and memory performance, and our data suggest that it may also be the link to understanding the relationship between neocortical amyloid and memory performance. We observed that entorhinal tau only weakly mediated the association between neocortical amyloid and memory performance, which suggests that entorhinal tau and neocortical amyloid are independent processes in the earliest stages of the disease.[2] This is consistent with recent reports of independent and atrophy-mediated relationships between local tau and memory performance.[27,28] However, when presubiculum volumes are lower, both increased entorhinal tau volume and lower presubiculum volume together constitute the underlying pathologies accompanying neocortical amyloid-associated memory performance and thus

Table 2 Mediation statistics

	β	Wald *z* score	*p* Value	Bootstr 95% CI
EC tau mediating neocortical amyloid and memory				
Path a: PiB → EC	0.464	4.49	<0.001	0.261 to 0.666
Path b: EC → MEM	−0.182	−2.13	0.033	−0.350 to −0.015
Indirect effect (a × b)	−0.085	−1.91	0.056	−0.171 to 0.002
Direct effect c′: PiB → MEM	−0.125	−1.28	0.201	−0.317 to 0.067
Presubiculum volume mediates neocortical amyloid—memory (via EC tau)				
Path a: PiB → EC	0.464	4.49	<0.001	0.261 to 0.666
Path b: EC → MEM	−0.121	−1.35	0.179	−0.296 to 0.055
Path a2: EC → Presub	−0.283	−3.19	0.001	−0.456 to −0.109
Path b2: Presub → MEM	0.272	3.83	<0.001	0.133 to 0.411
Indirect effect (presub via EC)	−0.036	−2.05	0.040	−0.070 to −0.002
Direct effect c′: PiB → MEM	−0.138	−1.38	0.167	−0.333 to 0.058
Hippocampal amyloid moderates the relationship between EC tau and presubiculum volume in the mediation model of presubiculum volume (via EC tau) on neocortical amyloid—memory				
Path a: PiB → EC	0.464	4.49	<0.001	0.261 to 0.666
Path b: EC → MEM	−0.115	−1.31	0.190	−0.287 to 0.057
Path a2: EC → Presub	−0.264	2.56	0.010	−0.427 to −0.099
Path d1: Hipp ab × EC → Presub	−0.690	−3.04	0.002	−0.264 to −0.057
Path b2: Presub → MEM	0.238	2.87	0.004	0.076 to 0.402
Conditional indirect effect				
Hipp ab: mean − 1 SD	−0.077	−1.03	0.305	−0.085 to 0.028
Hipp ab: mean	−0.097	−1.83	0.068	−0.139 to 0.005
Hipp ab: mean + 1 SD	−0.118	−2.04	0.042	−0.207 to −0.004
Direct effect c′: PiB → MEM	−0.134	−1.37	0.170	−0.326 to 0.058
Entorhinal amyloid moderates the relationship between EC tau and presubiculum volume in the mediation model of presubiculum volume (via EC tau) on neocortical amyloid—memory				
Path a: PiB → EC	0.465	4.48	<0.001	0.311 to 0.620
Path b: EC → MEM	−0.110	−1.27	0.205	−0.285 to 0.064
Path a2: EC → Presub	0.518	1.91	0.055	−0.017 to 1.514
Path d1: EC ab × EC → Presub	−1.014	−2.62	0.009	−1.306 to −0.723
Path b2: Presub → MEM	0.344	2.89	0.004	0.218 to 0.818
Conditional indirect effect				
EC ab: mean − 1 SD	−0.072	−1.77	0.077	−1.083 to 0.055
EC ab: mean	−0.100	−1.75	0.079	−1.355 to 0.075
EC ab: mean + 1 SD	−0.129	−1.74	0.081	−1.627 to 0.095
Direct effect c′: PiB → MEM	−0.133	−1.38	0.168	−0.321 to 0.054

Abbreviations: ab = amyloid deposition; β = standardized coefficient estimate; Bootstr = bootstrap; CI = confidence interval; EC = entorhinal cortex tau; Hipp = hippocampal; MEM = memory; PiB = neocortical amyloid deposition; presub = presubiculum.
Mediation analyses were performed with bias-corrected bootstrapping at 5,000 iterations. All models are corrected for age, sex, and education. For the final model, the indirect effect was calculated at specific values of the moderator.

Figure 4 Alternative mediation model

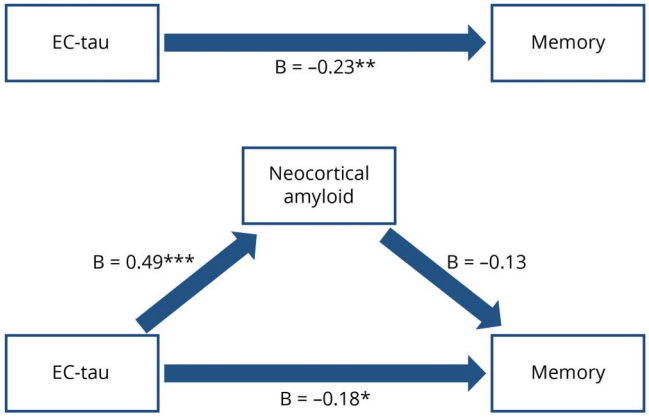

Top part shows the total effect of entorhinal tau on memory; lower part shows the mediation by neocortical amyloid. There was no significant indirect effect (β = −0.06, t = −1.28, p = 0.20). All β values are standardized estimates. EC = entorhinal cortex. *p < 0.05; **p < 0.01; ***p < 0.001.

memory performance in the context of preclinical AD. This suggests that at this stage, when amyloid and tau pathology reached the hippocampus, neurodegeneration and amyloid are no longer independent processes.

The pathology underlying volume loss in the presubiculum remains unclear. Neuropathologic studies indicated that there is little neuronal loss in the presubiculum and that tau pathology occurs mainly in the presubiculum around neurofibrillary tangle stage IV to V, after other parts of the hippocampus such as CA1 are affected.[3,16,29,30] Amyloid pathology is another important pathology potentially contributing to presubiculum volume changes. While the distribution pattern of amyloid is characterized by considerable interindividual variability, it is important to note that at Thal phase 2 amyloid pathology (hippocampus and entorhinal cortex) can be detected in >50% of the individuals. The fact that the mediation by entorhinal tau and presubiculum volume on the relationship between neocortical amyloid and memory was not dependent on entorhinal amyloid may be consistent with autopsy studies indicating that entorhinal tau and entorhinal amyloid are independent processes.[31,32] Clinicohistopathologic work also showed no relationship between entorhinal amyloid and cognition.[33] However, our mediation model was contingent on hippocampal amyloid, and higher levels of hippocampal amyloid and entorhinal tau contributed to presubiculum volume. The superficial or parvopyramidal layer of the presubiculum is a predilection site for amyloid pathology and remains devoid of tau pathology in these autopsy-confirmed cases of AD, although neuropil threads can be observed.[29,30] Notably, presubicular amyloid is unique; it is diffuse and nonfibrillar (it is not Congo red or thioflavin positive but can bind to PiB[34]), and these presubicular amyloid lakes can already be observed in Thal phase 1.[18] Presubicular amyloid is not associated with substantial cytoarchitectural changes but most likely stems from neuronal projections to the parvopyramidal layer and thus represents amyloid from neuronal origin.[35] Lack of neurofibrillary tangles and age-related volume differences in the presubiculum seem contradictory,

Figure 5 Comparison of effect sizes of the relevant biomarkers

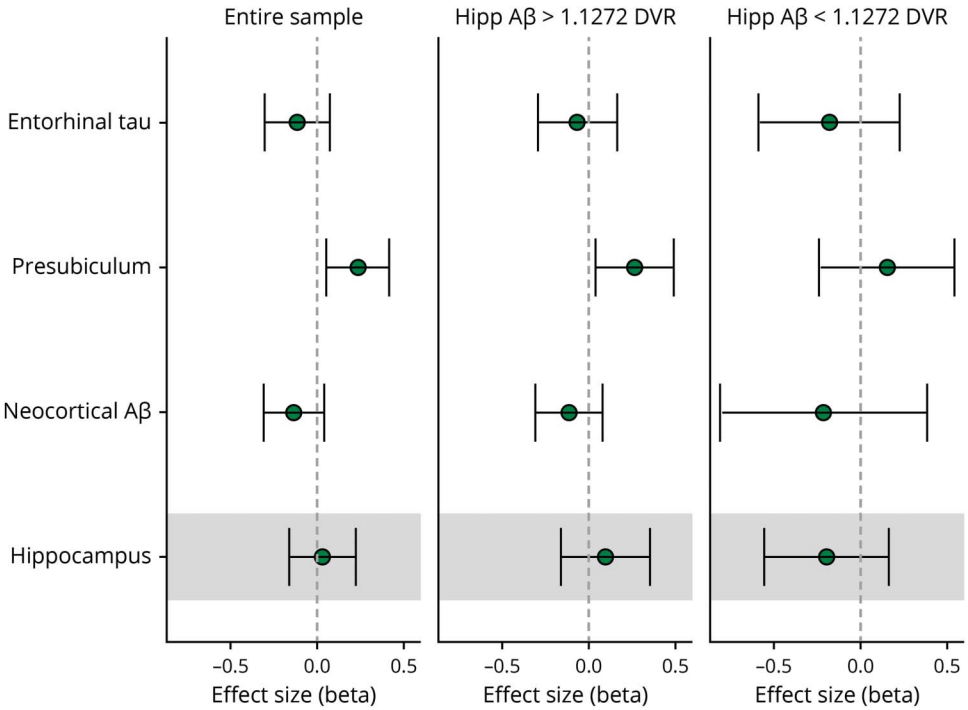

Effect sizes (standardized β coefficients) are plotted for the association between the markers and memory performance across the entire sample and individuals with lower or elevated levels of hippocampal (Hipp) amyloid (Aβ). Effect sizes reflect the magnitude of the association when all other markers are held constant. For comparison, the effect sizes between total hippocampal volume and memory performance are also shown (holding neocortical amyloid and entorhinal tau constant). DVR = distribution volume ratio.

but disruptions in such neuronal projections and other changes in components of the extracellular matrix can interact with amyloid protein accumulation and make neurons susceptible to shrinkage during early Braak stages.[36]

One of the most important pathways passing through the parvopyramidal layer of the presubiculum is the perforant pathway, part of the Papez circuit, which plays a vital role in episodic memory formation and storage.[2,37–40] It has been suggested that tau pathology propagates from the entorhinal cortex to hippocampal subregions via the perforant pathway.[37,39,41] While correlations between the perforant pathway and symptoms have often been related to morphologic changes in the dentate gyrus in individuals with dementia, perforant pathway—memory associations are likely of an axonal nature in the initial stages.[39] The perforant pathway crosses the presubiculum before reaching the other hippocampal subregions,[42] and hence, entorhinal tau and possibly other local MTL pathologic processes could disrupt information flow along the Papez ciruit.[43] This may explain why mediation through early neurodegenerative processes (entorhinal tau, presubiculum volume) explains amyloid-related memory performance when hippocampal amyloid is elevated, indicative of early Braak stage III. It can be speculated that presubiculum volume changes are a combination of reduced perforant pathway projections due to entorhinal tau and disrupted synaptic signal integration caused by local hippocampal amyloid or tau pathology.[44] The fact that this occurs at relatively low hippocampal amyloid levels (including a large proportion of the neocortical amyloid–negative individuals) suggests that these processes occur early in the disease process, possibly before accrual of significant pathology. Lower neocortical amyloid may be clinically relevant.[45]

Presubiculum volume loss may thus be related to functional deterioration processes increasing the progression of pathology and cognitive decline. These findings suggest that presubiculum volume may be a promising marker reflecting the earliest signs of imminent memory problems and possibly spread of pathology that is distinct from normal aging.

Identification of hippocampal subparts with FS 6.0 should be considered probabilistic because it uses prior knowledge from 15 ex vivo brains scanned at 7T MRI combined with the available contrast information from MRIs.[12] FS 6.0 has not yet been validated against manual segmentation or histology, and the ex vivo labeling was not at the histology resolution, which would have been required to identify all the strata. Furthermore, combining the contrast of a T2- with T1-weighted image improves the segmentation of FS (but see figure e-1, doi.org/10.5061/dryad.f33n0s8), but high-resolution T2-weighted images were not available for this dataset. A recent study showed high test-retest reliability using T1-weighted images in FS 6.0 among older individuals and patients with AD,[46] indicating that T1-based subregion segmentation provides useful information that is not conveyed in total hippocampal volume.[12]

To date, there is no consensus on the hippocampal subregion boundaries, which hinders quantitative comparisons across studies. A working group is developing a harmonized protocol that will facilitate comparisons across samples and laboratories (hippocampalsubfields.com).[47] Contradictory to other, mainly patient, studies,[10] we did not find an association between CA1 volume and memory. The review of the work by de Flores et al.[10] revealed heterogeneity between aging studies, likely because of differences in age span, sample size, methodology, or inclusion of biomarker or genetic risk information. In comparisons of the volumes of the subiculum, the CA1, and the rest of the hippocampus using voxel-based morphometry methods, the subiculum was most sensitive to aging.[48] The border between the CA1 and subiculum shows the highest variability across segmentation protocols.[49] In many of these protocols, the potential of the presubiculum as a marker for early detection of AD may have gone unnoticed because it is not segmented. FS parcellates the hippocampus into >10 substructures, including the presubiculum, which is localized on the lower bank of the hippocampal sulcus. Regardless of the specific parcellation protocol of the hippocampus, our finding about presubiculum volume concerns the inferior bank of the hippocampal sulcus. While efforts to improve and harmonize hippocampal subfield segmentation continue to evolve, it should be noted that FS 6.0 matches the histologic estimates[12,50] and is a widely used tool in neuroscience.

We focused specifically on MTL regions because these regions are particularly vulnerable to initial pathologic processes. We consider these results hypothesis generating, and future studies should expand to include neocortical tau regions to link these early MTL processes to the progression of pathology and disease stages.

Finally, while understanding the biomarker sequence is important to advance early detection of AD and to improve our knowledge of the pathophysiology of AD, it is important to highlight that all data were cross-sectional and observational, without any experimental manipulation. Our results add important information on relationships between early biomarkers, but our inferences remain correlational, and we cannot make any causality claims. Future longitudinal studies with sufficient time points and a broader range of value in amyloid PET, tau PET, structural MRI, and cognition will be able to test the proposed chain of events.

Presubiculum volume links initial signs of AD pathology to memory performance and may be a valuable marker reflecting the earliest signs of imminent memory problems, distinct from normal aging. Hippocampal amyloid strengthens the association between early tau and presubiculum volume, a region devoid of tau tangles or fibrillar amyloid, suggesting that amyloid is a necessary, but not sufficient, process to drive neurodegeneration in memory-related regions. Potential processes include alterations in structural connections or disrupted neuronal activity. Future longitudinal studies can provide insight into the biomarker sequence, and studies including brain

regions outside the MTL and clinically impaired samples will increase our understanding of the role of the presubiculum in the progression of pathology and its relation to memory decline.

Acknowledgment

The author thank Dr. Julie Price (Massachusetts General Hospital/Harvard Medical School) for valuable discussions on the use and interpretation of the temporal signal-to-noise ratio metric.

Study funding

This work was supported in part by the Athinoula A. Martinos Center for Biomedical Imaging P41 EEB015896 and shared instrumentation grants S10RR021110, S10OD010364, S10RR023401, S10RR023043, and 1S10RR019307. The research was supported in major part by the HABS (P01 AG036694). H. Jacobs received funding from Alzheimer Nederland (WE.15-2014-06). K. Papp is funded by National Institute on Aging grant K23 AG053422-01 and the Alzheimer's Association. K. Johnson received funding from NIH grants R01 EB014894, R21 AG038994, R01 AG026484, R01 AG034556, P50 AG00513421, U19 AG10483, P01 AG036694, R13 AG042201174210, R01 AG027435, and R01 AG037497; Alzheimer's Association grant ZEN-10-174210; the Harvard Neurodiscovery Center; and Fidelity Biosciences. R. Sperling receives research support from the following grants: P01 AG036694, U01 AG032438, U01 AG024904, R01 AG037497, R01 AG034556, K24 AG0350007, P50 AG005134, U19 AG010483, R01 AG027435, Fidelity Biosciences, Harvard NeuroDiscovery Center, and the Alzheimer's Association.

Disclosure

H. Jacobs and J. Augustinack report no disclosures relevant to this manuscript. A. Schultz has been a paid consultant for Janssen Pharmaceuticals and Biogen. B. Hanseeuw, J. Locascio, and R. Amariglio report no disclosures. K. Papp has served as a paid consultant for Biogen. D. Rentz has done consulting for Eli Lilly and served on the Scientific Advisory Board for Neurotrack. R. Sperling has served as a paid consultant for Abbvie, Biogen, Bracket, Genentech, Lundbeck, Roche, and Sanofi. She has served as coinvestigator for Avid, Eli Lilly, and Janssen Alzheimer Immunotherapy clinical trials. She has spoken at symposia sponsored by Eli Lilly, Biogen, and Janssen. R. Sperling receives research support from Janssen Pharmaceuticals and Eli Lilly and Co. K. Johnson has served as paid consultant for Janssen, Siemens Medical Solutions, Genentech, Novartis, Biogen, Roche, Lilly, Piramal, AZTherapy, Lundbeck, Merck, and Abbvie. He is a site coinvestigator for Lilly/Avid, Janssen Immunotherapy, and Pfizer. Go to Neurology.org/N for full disclosures.

Publication history

Received by *Neurology* December 23, 2018. Accepted in final form November 14, 2019.

Appendix Authors

Name	Location	Contribution
Heidi Jacobs, PhD	Massachusetts General Hospital, Boston	Designed and conceptualized study; analyzed the data; performed statistical analysis; drafted the manuscript for intellectual content
Jean Augustinack, PhD	Massachusetts General Hospital, Boston	Designed and conceptualized study; interpreted the data; revised the manuscript for intellectual content
Aaron Schultz, PhD	Massachusetts General Hospital, Boston	Major role in image processing; interpreted the data; revised the manuscript for intellectual content
Bernard Hanseeuw, MD, PhD	Massachusetts General Hospital, Boston	Interpreted the data; revised the manuscript for intellectual content
Joseph Locascio, PhD	Massachusetts General Hospital, Boston	Oversight of statistical analyses; interpreted the data; revised the manuscript for intellectual content
Rebecca Amariglio, PhD	Brigham and Women's Hospital, Boston, MA	Data acquisition; interpreted the data; revised the manuscript for intellectual content
Kathryn Papp, PhD	Brigham and Women's Hospital, Boston, MA	Data acquisition; interpreted the data; revised the manuscript for intellectual content
Dorene Rentz, PsyD	Brigham and Women's Hospital, Boston, MA	Interpreted the data; revised the manuscript for intellectual content
Reisa Sperling, MD	Brigham and Women's Hospital, Boston, MA	Interpreted the data; revised the manuscript for intellectual content
Keith Johnson, MD	Massachusetts General Hospital, Boston	Design and conceptualized study; interpreted the data; revised the manuscript for intellectual content

References

1. West MJ, Kawas CH, Stewart WF, Rudow GL, Troncoso JC. Hippocampal neurons in pre-clinical Alzheimer's disease. Neurobiol Aging 2004;25:1205–1212.
2. Lace G, Savva GM, Forster G, et al. Hippocampal tau pathology is related to neuroanatomical connections: an ageing population-based study. Brain 2009;132:1324–1334.
3. Braak H, Del Tredici K. The preclinical phase of the pathological process underlying sporadic Alzheimer's disease. Brain 2015;138:2814–2833.
4. Jacobs HIL, Hedden T, Schultz AP, et al. Structural tract alterations predict downstream tau accumulation in amyloid-positive older individuals. Nat Neurosci 2018;21:424–431.
5. Serrano-Pozo A, Qian J, Monsell SE, Frosch MP, Betensky RA, Hyman BT. Examination of the clinicopathologic continuum of Alzheimer disease in the autopsy cohort of the National Alzheimer Coordinating Center. J Neuropathol Exp Neurol 2013;72:1182–1192.
6. Hyman BT, Phelps CH, Beach TG, et al. National Institute on Aging-Alzheimer's Association guidelines for the neuropathologic assessment of Alzheimer's disease. Alzheimers Dement 2012;8:1–13.
7. Price JL, Morris JC. Tangles and plaques in nondemented aging and "preclinical" Alzheimer's disease. Ann Neurol 1999;45:358–368.
8. Delacourte A, David JP, Sergeant N, et al. The biochemical pathway of neurofibrillary degeneration in aging and Alzheimer's disease. Neurology 1999;52:1158–1165.
9. Lee CM, Jacobs HIL, Marquie M, et al. 18F-flortaucipir binding in choroid plexus: related to race and hippocampus signal. J Alzheimers Dis 2018;62:1691–1702.
10. de Flores R, La Joie R, Chetelat G. Structural imaging of hippocampal subfields in healthy aging and Alzheimer's disease. Neuroscience 2015;309:29–50.
11. Dale AM, Fischl B, Sereno MI. Cortical surface-based analysis, I: segmentation and surface reconstruction. Neuroimage 1999;9:179–194.

12. Iglesias JE, Augustinack JC, Nguyen K, et al. A computational atlas of the hippocampal formation using ex vivo, ultra-high resolution MRI: application to adaptive segmentation of in vivo MRI. Neuroimage 2015;115:117–137.
13. Johnson KA, Schultz A, Betensky RA, et al. Tau positron emission tomographic imaging in aging and early Alzheimer disease. Ann Neurol 2016;79:110–119.
14. Logan J, Fowler JS, Volkow ND, et al. Graphical analysis of reversible radioligand binding from time-activity measurements applied to [N-11C-methyl]-(-)-cocaine PET studies in human subjects. J Cereb Blood Flow Metab 1990;10:740–747.
15. Greve DN, Svarer C, Fisher PM, et al. Cortical surface-based analysis reduces bias and variance in kinetic modeling of brain PET data. Neuroimage 2014;92:225–236.
16. Braak H, Braak E. Neuropathological stageing of Alzheimer-related changes. Acta Neuropathol (Berl) 1991;82:239–259.
17. Thal DR, Rub U, Orantes M, Braak H. Phases of A beta-deposition in the human brain and its relevance for the development of AD. Neurology 2002;58:1791–1800.
18. Thal DR, Rub U, Schultz C, et al. Sequence of Abeta-protein deposition in the human medial temporal lobe. J Neuropathol Exp Neurol 2000;59:733–748.
19. Ikonomovic MD, Klunk WE, Abrahamson EE, et al. Post-mortem correlates of in vivo PiB-PET amyloid imaging in a typical case of Alzheimer's disease. Brain 2008;131:1630–1645.
20. Driscoll I, Troncoso JC, Rudow G, et al. Correspondence between in vivo (11)C-PiB-PET amyloid imaging and postmortem, region-matched assessment of plaques. Acta Neuropathol 2012;124:823–831.
21. Yamaguchi H, Hirai S, Morimatsu M, Shoji M, Nakazato Y. Diffuse type of senile plaques in the cerebellum of Alzheimer-type dementia demonstrated by beta protein immunostain. Acta Neuropathol 1989;77:314–319.
22. Bruno D, Grothe MJ, Nierenberg J, et al. A study on the specificity of the association between hippocampal volume and delayed primacy performance in cognitively intact elderly individuals. Neuropsychologia 2015;69:1–8.
23. Hayes AF. Beyond Baron and Kenny: statistical mediation analysis in the new millennium. Commun Monogr 2009;76:408–420.
24. Zeidman P, Lutti A, Maguire EA. Investigating the functions of subregions within anterior hippocampus. Cortex 2015;73:240–256.
25. Carlesimo GA, Piras F, Orfei MD, Iorio M, Caltagirone C, Spalletta G. Atrophy of presubiculum and subiculum is the earliest hippocampal anatomical marker of Alzheimer's disease. Alzheimers Dement (Amst) 2015;1:24–32.
26. Ding SL. Comparative anatomy of the prosubiculum, subiculum, presubiculum, postsubiculum, and parasubiculum in human, monkey, and rodent. J Comp Neurol 2013;521:4145–4162.
27. Bejanin A, Schonhaut DR, La Joie R, et al. Tau pathology and neurodegeneration contribute to cognitive impairment in Alzheimer's disease. Brain 2017;140:3286–3300.
28. Maass A, Lockhart SN, Harrison TM, et al. Entorhinal tau pathology, episodic memory decline, and neurodegeneration in aging. J Neurosci 2018;38:530–543.
29. Arriagada PV, Marzloff K, Hyman BT. Distribution of Alzheimer-type pathologic changes in nondemented elderly individuals matches the pattern in Alzheimer's disease. Neurology 1992;42:1681–1688.
30. Braak H, Braak E. The human entorhinal cortex: normal morphology and lamina-specific pathology in various diseases. Neurosci Res 1992;15:6–31.
31. Katsuno T, Morishima-Kawashima M, Saito Y, et al. Independent accumulations of tau and amyloid beta-protein in the human entorhinal cortex. Neurology 2005;64:687–692.
32. Thaker AA, Weinberg BD, Dillon WP, et al. Entorhinal cortex: antemortem cortical thickness and postmortem neurofibrillary tangles and amyloid pathology. AJNR Am J Neuroradiol 2017;38:961–965.
33. Mufson EJ, Chen EY, Cochran EJ, Beckett LA, Bennett DA, Kordower JH. Entorhinal cortex beta-amyloid load in individuals with mild cognitive impairment. Exp Neurol 1999;158:469–490.
34. Ji B, Chen CJ, Bando K, et al. Distinct binding of amyloid imaging ligands to unique amyloid-beta deposited in the presubiculum of Alzheimer's disease. J Neurochem 2015;135:859–866.
35. Wisniewski HM, Sadowski M, Jakubowska-Sadowska K, Tarnawski M, Wegiel J. Diffuse, lake-like amyloid-beta deposits in the parvopyramidal layer of the presubiculum in Alzheimer disease. J Neuropathol Exp Neurol 1998;57:674–683.
36. Bonneh-Barkay D, Wiley CA. Brain extracellular matrix in neurodegeneration. Brain Pathol 2009;19:573–585.
37. Ahmed Z, Cooper J, Murray TK, et al. A novel in vivo model of tau propagation with rapid and progressive neurofibrillary tangle pathology: the pattern of spread is determined by connectivity, not proximity. Acta Neuropathol 2014;127:667–683.
38. de Calignon A, Polydoro M, Suarez-Calvet M, et al. Propagation of tau pathology in a model of early Alzheimer's disease. Neuron 2012;73:685–697.
39. Thal DR, Holzer M, Rub U, et al. Alzheimer-related tau-pathology in the perforant path target zone and in the hippocampal stratum oriens and radiatum correlates with onset and degree of dementia. Exp Neurol 2000;163:98–110.
40. Kalus P, Braak H, Braak E, Bohl J. The presubicular region in Alzheimer's disease: topography of amyloid deposits and neurofibrillary changes. Brain Res 1989;494:198–203.
41. Hyman BT, Van Hoesen GW, Kromer LJ, Damasio AR. Perforant pathway changes and the memory impairment of Alzheimer's disease. Ann Neurol 1986;20:472–481.
42. Augustinack JC, Helmer K, Huber KE, Kakunoori S, Zollei L, Fischl B. Direct visualization of the perforant pathway in the human brain with ex vivo diffusion tensor imaging. Front Hum Neurosci 2010;4:42.
43. Garcia-Sierra F, Hauw JJ, Duyckaerts C, Wischik CM, Luna-Munoz J, Mena R. The extent of neurofibrillary pathology in perforant pathway neurons is the key determinant of dementia in the very old. Acta Neuropathol 2000;100:29–35.
44. Stern EA, Bacskai BJ, Hickey GA, Attenello FJ, Lombardo JA, Hyman BT. Cortical synaptic integration in vivo is disrupted by amyloid-beta plaques. J Neurosci 2004;24:4535–4540.
45. Bischof GN, Jacobs HIL. Subthreshold amyloid and its biological and clinical meaning: long way ahead. Neurology 2019;93:72–79.
46. Worker A, Dima D, Combes A, et al. Test-retest reliability and longitudinal analysis of automated hippocampal subregion volumes in healthy ageing and Alzheimer's disease populations. Hum Brain Mapp 2018;39:1743–1754.
47. Wisse LEM, Daugherty AM, Olsen RK, et al. A harmonized segmentation protocol for hippocampal and parahippocampal subregions: why do we need one and what are the key goals? Hippocampus 2017;27:3–11.
48. La Joie R, Fouquet M, Mezenge F, et al. Differential effect of age on hippocampal subfields assessed using a new high-resolution 3T MR sequence. Neuroimage 2010;53:506–514.
49. Yushkevich PA, Amaral RS, Augustinack JC, et al. Quantitative comparison of 21 protocols for labeling hippocampal subfields and parahippocampal subregions in in vivo MRI: towards a harmonized segmentation protocol. Neuroimage 2015;111:526–541.
50. Simic G, Kostovic I, Winblad B, Bogdanovic N. Volume and number of neurons of the human hippocampal formation in normal aging and Alzheimer's disease. J Comp Neurol 1997;379:482–494.